

## Development and Characterization of an In Vivo Central Venous Catheter *Candida albicans* Biofilm Model

D. Andes,<sup>1,2\*</sup> J. Nett,<sup>1</sup> P. Oschel,<sup>3</sup> R. Albrecht,<sup>3</sup> K. Marchillo,<sup>1</sup> and A. Pitula<sup>1</sup>

*Department of Medicine,<sup>1</sup> Department of Medical Microbiology and Immunology,<sup>2</sup>  
and Biological and Biomaterials Preparation, Imaging, and Characterization  
Laboratory, Department of Animal Science,<sup>3</sup> University of Wisconsin,  
Madison, Wisconsin*

Received 14 May 2004/Accepted 16 June 2004

**Biofilms represent a niche for microorganisms where they are protected from both the host immune system and antimicrobial therapies. Biofilm growth serves as an increasing source of clinical infections. *Candida* infections are difficult to manage due to their persistent nature and associated drug resistance. Observations made in biofilm research have generally been limited to in vitro models. Using a rat central venous catheter model, we characterized in vivo *Candida albicans* biofilm development. Time-course quantitative culture demonstrated a progressive increase in the burden of viable cells for the first 24 h of development. Fluorescence and scanning electron microscopy revealed a bilayered architecture. Adjacent to the catheter surface, yeast cells were densely embedded in an extracellular matrix. The layer adjacent to the catheter lumen was less dense. The outermost surface of the biofilm contained both yeast and hyphal forms, and the extracellular material in which they were embedded appeared fibrous. These architectural features were similar in many respects to those described for in vitro models. However, scanning electron microscopy also revealed host cells embedded within the biofilm matrix. Drug susceptibility was determined by using two assays and demonstrated a biofilm-associated drug resistance phenotype. The first assay demonstrated continued growth of cells in the presence of supra-MIC antifungal drug concentrations. The second assay demonstrated reduced susceptibility of biofilm-grown cells following removal from the biofilm structure. Lastly, the model provided sufficient nucleic material for study of differential gene expression associated with in vivo biofilm growth. Two fluconazole efflux pumps, *CDR1* and *CDR2*, were upregulated in the in vivo biofilm-associated cells. Most importantly, the studies described provide a model for further investigation into the molecular mechanisms of *C. albicans* biofilm biology and drug resistance. In addition, the model provides a means to study novel drug therapies and device technologies targeted to the control of biofilm-associated infections.**

Biofilms are structured microbial communities in which the microbial cells irreversibly attach to a surface or interface and become embedded in a matrix of extracellular polymeric substances produced by these cells (9, 13, 14, 15). Cells associated with this type of growth demonstrate phenotypic traits distinct from those associated with planktonic growth (3). Most notably, biofilm-associated cells demonstrate resistance to antimicrobial therapy (4, 8, 31, 34, 45). Recent estimates suggest that the majority of hospital-acquired infections are biofilm associated (15, 26, 42). Almost invariably, an implanted device such as an intravascular or urinary catheter or other medical device is associated with these infections. These medical devices have become an essential component in the supportive care of patients undergoing intensive medical and surgical treatments.

*Candida albicans* is the fourth leading cause of vascular catheter-related infections and the third leading cause of urinary catheter-related infections (6, 32, 38, 41). Among vascular catheter-related infections, those due to *Candida* spp. are associated with the highest rate of mortality (6, 10, 58). Successful therapy of these foreign-body infections can be a therapeutic challenge, requiring device removal in most instances (1, 12,

17, 24, 38, 51). Current guidelines for the treatment of candidemia and candiduria advocate removal of the associated device (41). However, removal of these devices is not always feasible, replacement is expensive, and in the case of central venous catheters, replacement is associated with a procedural risk to the patient.

Numerous investigations have been undertaken to characterize bacterial biofilms, in both the industrial and medical fields (9, 13, 14, 15, 31). More recently studies have begun to address fungal biofilms (2, 3, 4, 5, 8, 23, 24, 25, 34, 45, 46, 47). All studies of fungal biofilms thus far have involved in vitro test systems. These studies have identified several factors affecting *Candida* biofilm formation and have described a variety of phenotypic characteristics associated with this mode of growth (3, 4). The particular *Candida* species, nature of the device surface, presence of a host-derived conditioning film, and liquid flow have been shown to affect biofilm development (4, 8, 21, 23, 52). For example, the extent of biofilm matrix is increased when biofilms of *C. albicans* are incubated in vitro with gentle shaking, instead of statically, to produce the flow of liquid over the surface of the cells (4). However, because of the complexity of the milieu surrounding implanted prosthetic medical devices, such as intravascular catheters, it is difficult to accurately duplicate in vivo conditions in in vitro models. For example, despite attempts to introduce flow into an in vitro model, it is not possible to mimic the flow characteristics found

\* Corresponding author. Mailing address: University of Wisconsin, Departments of Medicine and Medical Microbiology Immunology, 600 Highland Ave., Room H4/572, Madison, WI 53792. Phone: (608) 263-1415. Fax: (608) 263-4464. E-mail: dra@medicine.wisc.edu.

in the host vasculature. In addition, there have been attempts to mimic the conditioning of intravascular devices by preinfection exposure to a variety of serum components such as fibrinogen (8). However, continuous exposure to these host proteins has not been accomplished in current *in vitro* models. In addition, it is not possible to include in these models each of the host proteins that are likely important *in vivo*. Perhaps most importantly, the host immune system and infection site have not been accounted for in these *in vitro* systems. It is thus desirable to test models of biofilm pathogenesis *in vivo*.

Several investigators have attempted to develop *in vivo* bacterial biofilm models to reflect the interaction between pathogens and devices to which they adhere (18, 19, 61). Most have placed either graft material, catheter segments, or tissue cages in the subcutaneous tissue. Unfortunately, features such as blood flow dynamics, serum proteins and other blood components, and humoral immunity are not accurately reflected in these models.

We propose that the availability of well-characterized, reproducible *in vivo* biofilm models will be essential to understanding the nature of this process in clinical infections. The present studies describe the development of an *in vivo* *C. albicans* model of venous catheter-associated biofilm.

#### MATERIALS AND METHODS

**Animals.** Specific-pathogen-free female Sprague-Dawley rats weighing 400 g (Harlan Sprague-Dawley, Indianapolis, Ind.) were used for all studies. Animals were housed in an environmentally controlled room with 12-h light-dark cycle and were maintained on a standard ad libitum rat diet. Animals were maintained in accordance with the American Association for Accreditation of Laboratory Care criteria (37). Animal studies were approved by the Animal Research Committee of the William S. Middleton Memorial Veterans Administration Hospital.

**Catheter.** The catheter diameter was chosen in an attempt to permit blood flow around the extraluminal catheter surface. The catheter tubing material was chosen to mimic a material used in patients. A polyethylene tubing from Intramedic met these criteria (PE 100 [inner diameter, 0.76 mm; outer diameter, 1.52 mm]; Intramedic catalog no. 427430; Becton Dickinson and Company, Franklin Lakes, N.J.).

The length of the catheter was determined based upon the sum of the planned intravascular distance (from the insertion in the internal jugular vein to above the right atrium) (2 cm), the subcutaneous tunneled distance, and the length of catheter to run in an external protective device from the animal to the cage top for ease of catheter access. These 50-cm segment lengths were gas sterilized with ethylene oxide prior to placement in the animals. The volume of this catheter length was determined to be 500  $\mu$ l.

**Catheter placement.** Prior to catheter surgery, the rats were anesthetized by intraperitoneal injection (1 mg/kg) of a mixture of xylazine (AnaSed; Lloyd Laboratories, Shenadonah, Iowa) (20 mg/ml) and ketamine (Ketaset; Aveco Co., Fort Dodge, Iowa) (100 mg/ml) in a ratio of 1:2 (vol/vol). Hair was shaved from the midscapular space, anterior chest, and neck. The rat was placed in the supine position; the surgical area was prepped and draped in a sterile fashion. A vertical incision was made in skin of the anterior neck just right of midline. The internal jugular vein was identified and exposed with blunt surgical dissection. A longitudinal incision of a few millimeters was then made to the vein wall with vein scissors. The heparinized (100 U/ml) catheter was placed in the opening and advanced to a site above the right atrium (approximately 2 cm). The catheter was secured to the vein with 3-0 silk ties. The proximal end of the catheter was then tunneled subcutaneously to the midscapular space and externalized through the skin via a button, which was secured with sutures. The anterior neck site was closed with surgical staples (Ethicon Endo-Surgery, Cincinnati, Ohio), and the midscapular button was secured with 2-0 Ti-cron suture. Recovery of the animal after the catheter surgery was assessed according to a standard protocol approved by the Veterans Administration Animal Committee.

**Animal and catheter maintenance.** The animals were examined for signs of distress every 8 h through the study. The anterior neck incision and the catheter exit site were examined twice daily for signs of inflammation or purulence. The catheters were flushed daily with heparinized (100 U/ml) 0.85% NaCl.

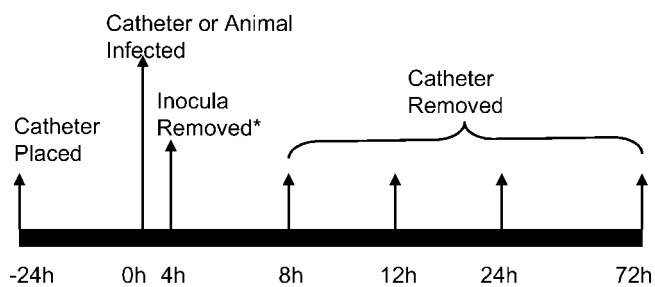


FIG. 1. Experimental time line of the *in vivo* rat catheter infection model.

**Organism and inoculum.** *C. albicans* K1 was used for all studies. The organism is a clinical isolate from a systemic *Candida* infection. The organism was maintained, grown, subcultured, and quantified on Sabouraud dextrose agar (SDA) plates (Difco Laboratories, Detroit, Mich.).

The organism was subcultured at 35°C on SDA 24 h prior to infection. The inoculum was prepared by placing three colonies into 5 ml of sterile pyrogen-free 0.85% NaCl warmed to 35°C. The final inoculum was adjusted to 5.60 log<sub>10</sub> CFU/ml via hemacytometer count. Viable fungal counts of the inoculum were confirmed by plating on SDA and were 5.54 to 5.74 log<sub>10</sub> CFU/ml.

**Infection.** A time course schematic of the experiment is shown in Fig. 1. The catheters were placed 24 h prior to infection to allow a conditioning period for deposition of host protein on the catheter surface. After the conditioning time period, 100  $\mu$ l of blood was obtained from the catheter and cultured to ensure sterility. The inoculum of *C. albicans* K1 was instilled in the catheter in a 500- $\mu$ l volume (the entire catheter volume). The inoculum was allowed to dwell for 4 h, after which the catheter volume was withdrawn and the catheter was flushed and locked with heparinized 0.85% NaCl. This infection was undertaken with 10 animals.

For two animals the catheter infection was attempted by injection of a 0.2-ml volume of a similar inoculum (5.82 log<sub>10</sub> CFU of *C. albicans* K1 per ml) via the rat tail vein 24 h after initial placement.

**Quantitative culture from catheter, peripheral blood, and kidney.** For the directly infected catheters, two animals were sacrificed by CO<sub>2</sub> asphyxiation at four time points (8, 12, 24, and 72 h) after the inoculum of *C. albicans* was removed. After sacrifice the catheter was aseptically removed from infected animals. One milliliter of sterile 0.85% NaCl was slowly flushed through the catheter to remove blood and nonadherent organisms. The distal 2 cm of catheter was cut from the entire catheter length, and the segment was placed in 1 ml of 0.85% NaCl in a 1.5-ml tube. The tube was sonicated for 10 min (FS 14 water bath sonicator and 40-kHz transducer [Fisher Scientific]) and vigorously vortexed for 30 s (43). Venous blood (100  $\mu$ l) was removed from the tail veins of animals at the same time points. To ascertain the extent of metastatic disease, the right kidney was also removed from each animal, placed in a volume of 0.85% NaCl to achieve an initial 1:10 dilution by weight, and homogenized. Following serial 1:10 dilution of the catheter fluid and kidney material, the samples were plated on SDA for viable fungal colony counts after incubation for 24 h at 35°C. The lower limit of detection was 100 CFU/ml or 100 CFU/kidney. Results were expressed as the mean CFU per milliliter or kidney from two mice.

The catheters from two distantly infected rats were removed 24 h after infection and processed similarly.

**Catheter biofilm imaging. (i) Confocal microscopy.** The distal 2 cm of catheter was further cut perpendicular to the catheter length with an 11-blade scalpel into three 2- to 3-mm-long "doughnut" segments. The catheter segments were stained with the FUN-1 (50  $\mu$ M) component of the LIVE/DEAD yeast viability kit (Molecular Probes, Eugene, Oreg.) and concanavalin A (ConA) conjugate (Alexa Fluor 488 conjugate) (200 mM) according to the manufacturer's instructions (20, 33). Both live and dead cells are labeled with this dye. All yeast cells are stained with the FUN-1 dye and visualized with a diffusely distributed green fluorescence. Metabolically active cells process this dye, which results in a shift from green to red fluorescence within intravacuolar structures. ConA binds to glucose and mannose residues of cell wall polysaccharides and is visualized as green fluorescence. Due to colocalization of fluorescent dyes (FUN-1 and ConA), the metabolically active cells appear yellow to orange during multichannel image capture. Prior study has demonstrated the utility of this dye pair for imaging of both the extracellular biofilm, which is made up largely of polysaccharides, and the associated cells simultaneously (8).

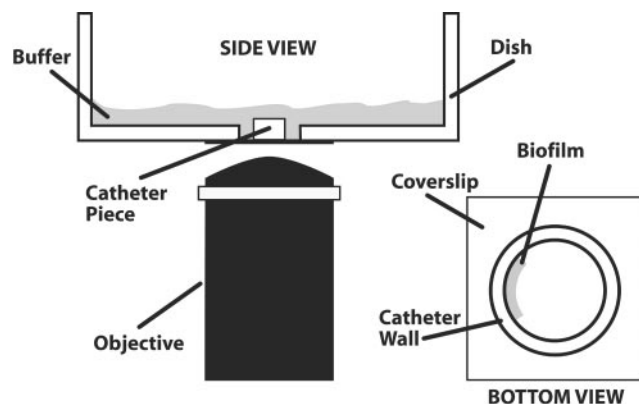


FIG. 2. Imaging setup for confocal microscopy of the catheter-associated biofilm.

Stained catheter segments were transferred to a glass-bottom petri dish (coverslip 1.5, 35-mm disk P325G 1.5-14C; MatTek, Ashland, Mass.) in an on-end orientation. Biofilms were observed with a Nipkow disk-based confocal microscope (Axiovert 200; Zeiss, Gottingen, Germany) equipped with a mercury arc lamp. The objectives used included 20 $\times$  and 40 $\times$  differential interference contrast oil immersion objectives. Depth measurements were taken at regular intervals across the biofilm. Confocal images of green (ConA) and red (FUN-1) fluorescence were conceived simultaneously using the Z-stack mode. A line drawing of the imaging procedure is shown in Fig. 2.

Imaging of FUN-1-stained cells was accomplished by using a protocol with an excitation wavelength of 488 nm and emission bands at 528 and 617 nm for green and red, respectively. The ConA protocol included excitation and emission wavelengths of 490 and 528 nm, respectively. Images were processed for display by using Axiovision 3.x software (Zeiss).

(ii) **Scanning electron microscopy.** Catheter disk segments were washed with phosphate-buffered saline and placed in fixative (1% [vol/vol] glutaraldehyde and 4% [vol/vol] formaldehyde) overnight. The samples were rinsed in 0.1 M phosphate buffer two times for 3 min each and then placed in 1% osmium tetroxide for 30 min, followed by immersion in hexamethyldisilazane (Polysciences, Inc., Warrington, Pa.). The samples were subsequently dehydrated in a series of ethanol washes (30% for 10 min, 50% for 10 min, 70% for 10 min, 95% for 10 min, and 100% for 10 min). Final desiccation was accomplished by critical-point drying (Tousimis, Rockville, Md.). Specimens were mounted on aluminum stubs and sputter coated with gold. Samples were observed in a scanning electron microscope (Hitachi S-5700) in the high-vacuum mode at 10 kV. The images were processed for display by using Adobe Photoshop version 5.0.

**Candida biofilm drug susceptibility in vivo.** Three assays were used to determine the fluconazole susceptibility phenotype of in vivo biofilm-associated cells compared to that of planktonically grown cells.

The first experiment compared in vivo growth of *C. albicans* in the presence and absence of the triazole fluconazole. Two catheters were placed in rats, and the catheters were directly infected as described above. After a period of biofilm growth (18 h), fluconazole was instilled and allowed to dwell in the catheter at a concentration of 8  $\mu$ g/ml, which is 16 times the planktonic MIC, for 5 h. After the 5 h, the 500- $\mu$ l catheter volume was removed and the same volume of sterile 0.85% NaCl was instilled. Another animal and indwelling catheter were similarly processed, except sterile 0.85% NaCl was used in place of fluconazole. The catheters were removed from the animals 1 h after drug removal. The catheters were flushed with sterile 0.85% NaCl to remove blood and nonadherent *C. albicans*. The distal 2 cm of the catheters, representing the intravascular length, was placed in sterile 0.85% sterile saline, sonicated, and quantitatively cultured as described above.

We similarly compared the viability of biofilm-associated cells after drug exposure and that of a no-drug control by using confocal imaging and FUN-1 vital staining of small catheter doughnuts as described above. We counted the number of cells with red fluorescence (metabolically active) per field (magnification,  $\times$ 40) for both fluconazole-treated cells and NaCl-treated control cells. We examined two catheter doughnuts per catheter and five microscopic fields per segment.

In a second experiment, we performed in vitro susceptibility testing with fluconazole on cells removed from an in vivo biofilm. The catheterized rat was

infected via the catheter as described above. After a 24-h period of biofilm development, the catheter was removed. The entire catheter was flushed with 0.85% NaCl, and the distal 2 cm was placed in 1 ml of 0.85% NaCl. The tube was then sonicated and vortexed to dislodge cells. The cells obtained after vortexing of the biofilm-involved catheter were used as the inoculum in a standard broth microdilution in vitro susceptibility test. The cells were quantified by hemacytometer count and transferred to a 96-well microtiter plate for susceptibility testing by the NCCLS M27-A method (36). The cell counts from hemacytometer measurements were confirmed by direct plating. The MIC for these cells was compared to that for planktonically grown cells. MIC determinations were performed in duplicate. Final results are expressed as the mean of these results.

**Transcriptional profile of biofilm-associated cells.** The mRNA abundances of four genes that have been shown to be associated with fluconazole drug resistance were measured both in the in vivo biofilm model and in planktonically grown *C. albicans* K1 (59). For collection of the in vivo biofilm-associated cells, the distal 2 cm of catheter after 24 h of biofilm development was utilized. The catheter segment was cut into multiple 2- to 3-mm-thick doughnuts and placed in 400  $\mu$ l of Tris-EDTA buffer. The tube containing the segments was sonicated and vortexed as described above. We next proceeded with total RNA isolation by the hot-phenol method of Schmitt et al. (53). For the comparative in vitro reference, cells were grown in yeast nitrogen base with shaking at 35 $^{\circ}$ C to an optical density at 600 nm of 0.6. The quantity of the RNA was determined via spectrophotometry with an ND-1000 spectrophotometer (NanoDrop Technologies, Montchanin, Del.).

**Quantitative RT-PCR.** Quantitative real-time reverse transcription-PCR (RT-PCR) was used to compare mRNA abundances of the genes of interest (7). The TaqMan MGB probe and primer sets were designed for the target genes *CDRI*, *CDR2*, *MDR1*, and *ERG11* and for the normalizing gene *ACT1* of *C. albicans* (Table 1), using Primer Express 1.5 software (Applied Biosystems, Foster City, Calif.). All probes have 6-carboxyfluorescein as a 5' fluorophore and 6-carboxytetramethylrhodamine as a 3' quencher (28). Primers annealed at 60 $^{\circ}$ C and defined the endpoints of the amplicon. Probes annealed at 70 $^{\circ}$ C and hybridized between, but not overlapping, the two endpoint primers. Oligonucleotides were synthesized by Integrated DNA Technologies (Coralville, Iowa).

The QuantiTect probe RT-PCR kit (Qiagen, Valencia, Calif.) was used in an ABI PRISM 7700 v1.7 sequence detection system (Applied Biosystems). Reactions were performed in duplicate according to the kit manufacturer's instructions. Final concentrations or amounts in the 50- $\mu$ l reaction included 1 $\times$  QuantiTect probe RT-PCR master mix, 1  $\mu$ M forward primer, 1  $\mu$ M reverse primer, 0.2  $\mu$ M probe, 1 U of heat-labile uracil-N-glycosylase, 0.5  $\mu$ l of QuantiTect probe RT mix, and 50 ng of total RNA. The ABI PRISM 7700 sequence detection system was programmed to reverse transcribe RNA at 50 $^{\circ}$ C for 30 min, followed by 15 min of initial HotStart Taq DNA polymerase activation at 95 $^{\circ}$ C. Two-step cycling, at 94 $^{\circ}$ C for 15 s and 60 $^{\circ}$ C for 1 min, was used for cDNA amplification. Fluorescence data were collected during the 60 $^{\circ}$ C annealing and extension step.

The quantitative data analysis was completed using the  $\Delta C_t$  ( $2^{-\Delta\Delta C_t}$ ) method of Livak and Schmittgen (27). For each amplification run, the threshold cycle,  $C_t$ , of the target was normalized to the  $C_t$  of the *ACT1* gene and related to the  $C_t$  of the control or baseline condition. The comparative  $\Delta C_t$ ,  $\Delta\Delta C_t$ , was defined as the difference between the  $\Delta C_t$  values:  $\Delta\Delta C_t = (C_{t, \text{target}} - C_{t, \text{normalizer}}) - (C_{t, \text{baseline}} - C_{t, \text{normalizer}})$ . The comparative expression value was transformed to an absolute value by using the following formula: fold change =  $2^{-\Delta\Delta C_t}$ .

The comparative expression method generated data as fold change in gene expression normalized to a constitutive reference gene and relative to a control or baseline condition. The statistical significance of differences in expression between biofilm and planktonic cells was analyzed by analysis of variance. The baseline condition in this case was mRNA isolated from planktonically grown *C. albicans* K1 cells. Real-time quantitative RT-PCR was performed on four 10-fold cDNA dilutions to ensure similar primer efficiencies among the various amplified targets (data not shown).

## RESULTS

**General animal well-being and catheter site observations.** The catheterized animals appeared well over the 96-h period of study (24 h preinfection and up to 72 h postinfection). Both the surgical site and catheter exit site remained free of signs of inflammation or purulence in all animals studied.

**Quantitative culture from catheter, peripheral blood, and kidney.** Time course viable counts from the catheter, rat kidney, and peripheral blood are shown in Fig. 3. At the first time

TABLE 1. *C. albicans* K1 primer combinations used in quantitative real-time RT-PCR<sup>a</sup>

Gene	Amplicon size (bp)	Primer	Primer sequence <sup>b</sup>	Start coordinate <sup>c</sup>	Accession no.
<i>CDR1</i>	70	Forward	5' CCATTAACCATCAGCACTTA	3174	X77589
		Reverse	5' CCGTTCTACCACCTTTTGTCA	3244	
		Probe	5' AGTCTATCAAACCTCAGCCA	3197	
<i>CDR2</i>	72	Forward	5' CACATGTCCGACATACCTGG	312	U63812
		Reverse	5' GGAATCTGGGTCTAATTGTTTCATGA	384	
		Probe	5' CCATTCAACGGCAACAT	340	
<i>MDR1</i>	61	Forward	5' GGTGCTCCTTTGTTTGACAATTT	1543	Y14703
		Reverse	5' ACGGAACTACCCCAAGCAACT	1604	
		Probe	5' CACCCCTGAATATC	1569	
<i>ERG11</i>	79	Forward	5' TCATTATTGGAGACGTGATGCTG	723	AF152848
		Reverse	5' GAAAGAAATTAACCTGAGAAGAGAACGTG	802	
		Probe	5' CAAAAGAAAATCTCTGCTACTTA	748	
<i>ACT1</i>	66	Forward	5' AGCTTTGTTTCAGACCAGCTGATT	779	X16377
		Reverse	5' TTGACCAAACCACTTTCAACTCC	845	
		Probe	5' CCAGCAGCTTCCAAACCT	803	

<sup>a</sup> RT-PCRs were run on an ABI PRISM 7700 v1.7 sequence detection system.

<sup>b</sup> All probes have 6-FAM as a 5' fluorophore and TAMRA as a 3' quencher. Primers and probes were designed by Primer Express 1.5; TaqMan MGB probe and primer design were used.

<sup>c</sup> Primer coordinates are determined by 5' base pair location in gene.

point (8 h) there were more than 3 log<sub>10</sub> CFU of viable cells per ml present on the 2-cm catheter segment. The burden of organisms associated with the biofilm and in the distant rat kidney continued to increase over the 72-h period of study. However, the majority of the maximal burden of viable cells was present in the first 24 h. The burden of organisms on the 2-cm length of catheter increased nearly 1 log<sub>10</sub> unit from our initial measurement at 8 h to the 24-h time point. Over the same period of time the organisms grew 1.5 log<sub>10</sub> units in the rat kidney, suggesting a somewhat slower rate of growth within the biofilm than at a distant organ site of metastasis. Culture of 100 μl of peripheral blood was not able to detect growth of *Candida* at any of the time points. However, growth of organisms in the kidney demonstrates the disseminated nature of

this infection model. The distantly (tail vein) infected catheter contained a similar burden of viable cells at the 24-h time point (4.50 log<sub>10</sub> CFU/ml).

**Catheter biofilm imaging. (i) Confocal microscopy.** Representative images of the intraluminal in vivo biofilms at magnifications of ×20 and ×40 in catheters after 24 h of development are shown in Fig. 4. The catheter and biofilm orientation is end on, with the catheter wall at the top left and the catheter lumen at the bottom right of the image. The thickness of the biofilm at maturity varied from 25 to nearly 200 μm on the intraluminal surface. The density of the biofilm matrix adjacent to the catheter wall makes it difficult to discern individual yeast cells. The hazy green appearance represents the dense extracellular material adjacent to the catheter wall. At the 8- and 12-h time points it is possible to visualize the outlines of individual cells adjacent to the catheter wall. In the mature (24- and 72-h) biofilm, distinct, metabolically active cells (stained yellow or red) and the surrounding extracellular matrix strands are visualized adjacent to the catheter lumen. Figure 4B clearly demonstrates only metabolically active cells utilizing only single-filter capture.

We did not capture the initial attachment of cells to the catheter with our earliest examination time point. By the 8-h time point (not shown), the biofilm was multiple cell layers thick, consisting of both yeast and hyphae. Fully mature biofilms were produced after 24 h and consisted of a dense network of yeasts, hyphae, and pseudohyphae. While the organisms continued to proliferate through the 72-h time point, the dimensions of the biofilm appeared similar to those at 24 h. At maturation the cells are completely encased within the matrix material. At this stage, focus on individual cells is difficult due to the matrix density.

Confocal imaging of the biofilm from the hematogenously infected catheter appeared similar to that for those infected intraluminally, except there was more biofilm on the extralu-

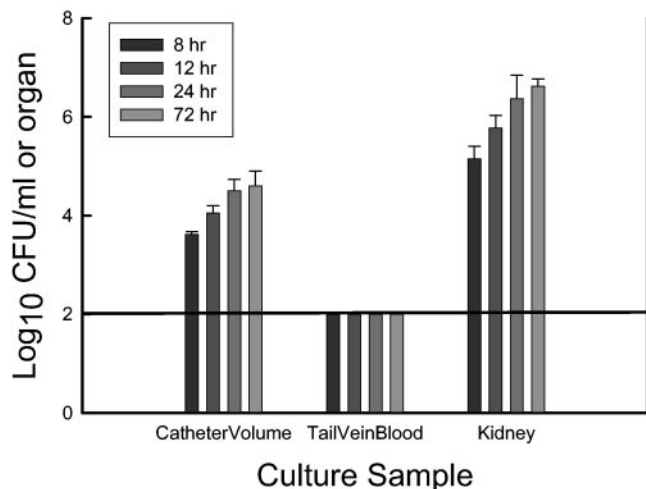


FIG. 3. Time course burden of viable *Candida* cells from the peripheral blood, sonicated catheter, and rat kidney. Bars represent means of data from two animals. Error bars represent standard deviations. The solid horizontal line represents the lower limit of detection.

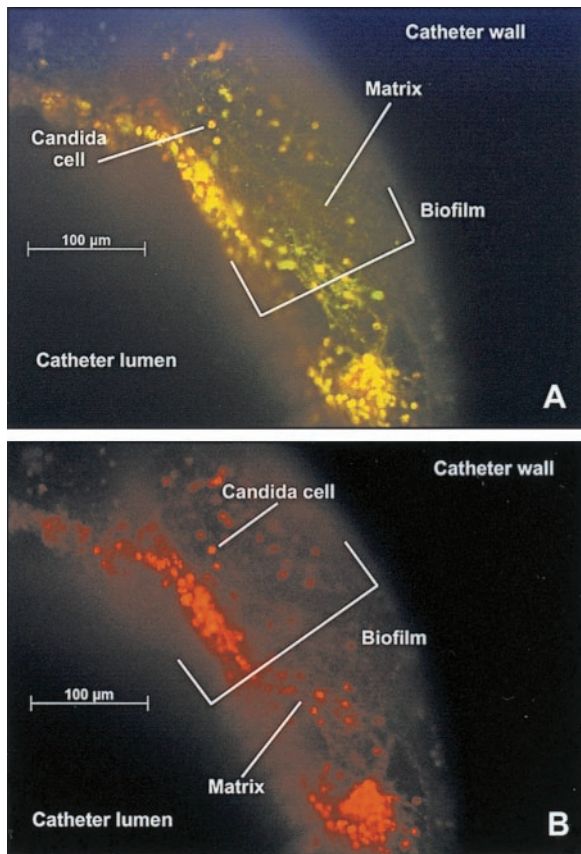


FIG. 4. Fluorescence images of in vivo *C. albicans* biofilm with both FUN-1 and ConA stains after 24 h of development. A view of the catheter wall and intraluminal biofilm in an end-on orientation is shown. Magnification,  $\times 20$ . (A) Image capture was set for simultaneous visualization of both green and red fluorescence. (B) Image capture was set for visualization of red fluorescence. Cells fluorescing red are metabolically active.

minimal surface (not shown) than with catheters infected via direct catheter dwelling of inoculum.

(ii) **Scanning electron microscopy.** Imaging of the biofilm on the catheter segments by scanning electron microscopy more clearly demonstrates the heterogeneous architecture of the biofilm structure. In Fig. 5A, the biofilm is imaged from above the intraluminal biofilm surface. The mature biofilm surface adjacent to the catheter lumen is characterized by both yeast and hyphal cell forms and a network of extracellular matrix strands. In Fig. 5B, the catheter segment is on end, and one can observe the differences between the biofilm adjacent to the wall of the catheter and that on the luminal surface. The basal region consists of densely packed yeasts encased in and often obscured by a surrounding extracellular material. Hyphal structures are also apparent in the basal region; however, they are fewer in number. Adjacent to the lumen, it is easier to discern yeast and hyphal forms, and the matrix is more strand-like and less compacted. In addition, scanning electron microscopy identified cell structures too large to represent *C. albicans*. We theorize, based on size, that these cells represent host neutrophils. Future study utilizing specific histochemical staining will be necessary to further identify these cell types. The

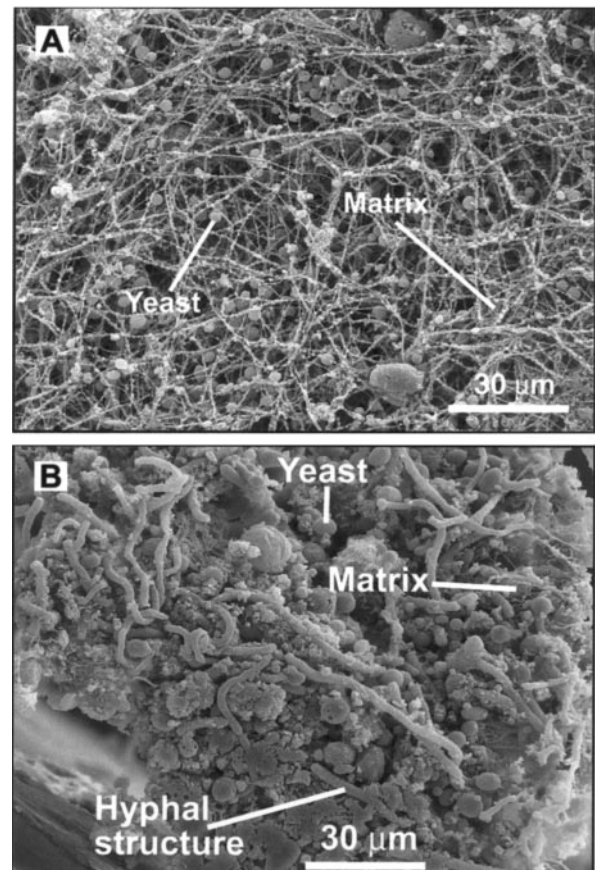


FIG. 5. Scanning electron microscopy image of in vivo *C. albicans* biofilm after 24 h of development. (A) View of intraluminal surface of biofilm; (B) view of biofilm cross-section.

proximity of the host cells within the biofilm points to the relevance of examination of this process in an in vivo system to capture the host-microbe-biofilm interaction.

***Candida* biofilm drug susceptibility in vivo.** In vivo exposure to fluconazole concentrations many times greater than the in vitro MIC did not impact *Candida* viability in mature biofilms. The drug-treated catheter contained a similar number of viable cells as determined by both quantitative culture (fluconazole,  $5.05 \log_{10}$  CFU/ml; NaCl,  $4.98 \log_{10}$  CFU/ml) and vital staining (fluconazole,  $25 \pm 5$  cells/ $40\times$  field; NaCl,  $27 \pm 8$  cells/ $40\times$  field).

We observed a remarkable rise in the MIC for cells associated with the in vivo biofilm compared to those grown planktonically. The traditional (planktonic) MIC of fluconazole in *C. albicans* K1 is  $0.5 \mu\text{g/ml}$ . The MIC for the cells recovered from the catheter was more than 128 times higher than the planktonic MIC ( $>64 \mu\text{g/ml}$ ).

**Transcriptional profile of biofilm-associated cell.** RNA isolation from a single catheter yielded enough material for numerous quantitative real-time RT-PCR experiments. More than 1,000 ng of total *C. albicans* RNA was isolated from a single catheter (260/280 ratio, 2.11). The fold change in abundance of genes examined from the biofilm relative to those from planktonic cells is shown in Fig. 6. The mRNA abundance of the gene encoding the drug target enzyme, *ERG11*, was not

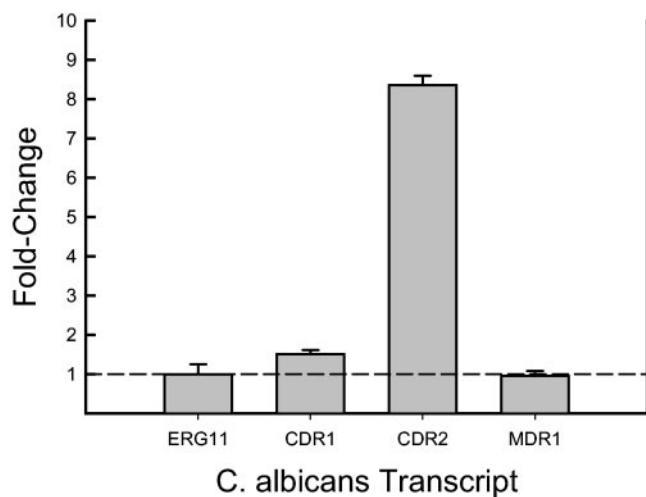


FIG. 6. mRNA abundances of selected genes (*ERG11*, *CDR1*, *CDR2*, and *MDR1*) from biofilm-associated *C. albicans* cells (after 24 h of development) compared to planktonically grown cells (optical density at 600 nm of 0.6). The height of the bars represents the ratio or fold change in expression of biofilm versus planktonic cells. Bars represent data from two RT-PCR replicates. Error bars represent standard deviations.

different between the planktonic and the in vivo biofilm-associated cells. Similarly, expression of the major facilitator pump, *MDR1*, did not appear to be remarkably affected by biofilm growth in vivo. However, mRNAs from both of the ATP-binding cassette pumps, *CDR1* and *CDR2*, were increased in the biofilm state ( $P < 0.01$ ). *CDR2* was the most remarkably affected, with a nearly 10-fold increase in expression. The results from RT-PCR were extremely similar in assay replicates.

## DISCUSSION

The incidence of systemic nosocomial infection due to *Candida* spp. has continued to increase over the past several decades (6, 22, 30, 41, 58). Despite antifungal therapy, the mortality of patients with invasive *Candida* infections remains high. Numerous studies have suggested that many if not most episodes of candidemia are catheter related (1, 24, 38, 50, 57). The largest prospective treatment study of candidemia implicated a catheter in 72% of patients (50). Predisposing factors for *Candida* infections include immunosuppressive therapy, antibiotic therapy, use of indwelling devices such as intravenous catheters, diabetes, and advanced age (1, 22, 30, 38, 39). The increase in *Candida* infections in the past two decades parallels the increased and widespread use of a broad range of medical devices. Biomaterials such as stents, shunts, prostheses (voice, heart valve, knee, etc), implants (lens, breast, denture, etc), endotracheal tubes, pacemakers, and catheters have all been shown to support colonization and biofilm infection by a variety of microorganisms, including *Candida* spp. In a prospective study of catheter colonization, *C. albicans* ranked second in the ratio of colonization to invasive disease (11).

The pathogenesis of these catheter-related *Candida* infections is complex. A variety of factors have been shown to be important in pathogenesis, including the duration of catheter placement, type of catheter material, and organism properties

(10). The source of organisms may include the skin, infusate, or endogenous sites, with the latter most commonly involving a breach of the gastrointestinal tract (10). Various imaging techniques have demonstrated that microorganisms in these infections grow in a biofilm environment. In fact, electron microscopy has suggested that biofilm-associated microorganisms can be found on most if not all central venous catheters (44). Biofilms thus pose an important public health problem for persons requiring the use of intravascular and other medical devices.

Biofilms are surface-attached microbial communities with characteristic architecture and with phenotypic properties distinct from those of their free-swimming, planktonic counterparts (9, 13, 15, 42). The organisms associated with biofilm growth are tenaciously attached to the underlying surface and biofilm matrix. The biofilm matrix is composed of microorganisms and a network of extracellular polymers produced by the involved microbes. One of the best known distinguishing characteristics of these biofilm-specific properties is the development of antimicrobial resistance that can be up to 1,000-fold greater than that of planktonic cells (31). This characteristic of biofilms makes them extremely difficult if not impossible to control in the medical setting. Studies of catheter-related *Candida* infection have shown that retention of vascular catheters colonized with *Candida* species is associated with prolonged fungemia, high antifungal therapy failure rates, an increased risk of metastatic complications, and death (1, 12, 17, 24, 30, 39, 51). In a multicenter study of 427 patients with candidemia, the mortality associated with catheter-related candida bloodstream infection was 41% in patients in whom the vascular catheter was retained (38).

Biofilms have been studied in a wide range of scientific disciplines, including biomedicine, water engineering, and evolutionary biology (9, 13, 15, 42). Examination of the pathogenesis of fungal biofilms has been more recently undertaken (2, 3, 4, 5, 8, 23, 25, 34, 45, 46, 47, 48). The methods used to study fungal biofilms have been limited to in vitro models. An immense amount of important data defining variables important for biofilm development and drug resistance has emerged from these studies. The factors shown to be important for biofilm development thus far include the *Candida* species, the nature of the device substrate, liquid flow, and a host-derived conditioning film covering the device surface (4, 8, 21, 23, 52). While in vitro studies have incorporated flow and surface conditioning into models, it would be extremely difficult to accurately mimic these important environmental factors. In addition, it is probable there are additional host variables contributing to biofilm development. Among the properties of the biofilm matrix that are theorized to be important for microorganism survival are the resistance to environmental insults from anti-infective drugs and the host immune system. Current in vitro models do not account for the interaction between the biofilm, host cells, and various other components of host immunity. Thus, a logical and necessary next step is to develop in vivo biofilm models to further our understanding of this important process in patients. The present paper describes an attempt to mimic a central venous catheter biofilm infection with *C. albicans* by using an in vivo rat animal model.

Comparison of results from the present in vivo study with those from several in vitro systems demonstrates both similar-

ities and differences. Imaging studies demonstrated an organized three-dimensional structure consisting of a dense network of yeasts and filamentous cells embedded in an extracellular matrix similar to that observed in vitro (8). However, the maximal thickness of the biofilm matrix observed in vivo was greater than that observed in vitro. Chandra et al. described a biofilm thickness of 25  $\mu\text{m}$  on biofilm formed on denture acrylic in vitro (8). Using a "kinetic" in vitro model, however, Ramage et al. reported a biofilm thickness nearly threefold greater at 70  $\mu\text{m}$  (49). The thickness of many areas of biofilm in this in vivo catheter model exceeded 100  $\mu\text{m}$ . This difference in thickness may be related to the time allowed for incubation or adherence (90 h in vitro and 4 h in the present model). Similar to descriptions in vitro, the rate of organism growth among biofilm-associated cells was reduced compared to that of cells not associated with biofilms (3). The increase in numbers of viable *Candida* cells in the kidneys of the rat was greater than that in the biofilms over the 8- to 72-h period of observation (1.5 versus 0.98  $\log_{10}$  CFU/kidney or CFU/ml). The biofilm growth progressed over the entire observation period; however, architectural maturity in vivo occurred within the first 24 h of development. In vitro, time course studies show biofilm maturity at 38 to 72 h (8). In addition, at earlier time points in vitro (8 to 11 h) the biofilm development is described as limited to adherent cells up to a few cell layers thick (8). In contrast, at the earliest point of observation in the present in vivo experiment, the process was several cell layers thick and the surrounding matrix could be visualized. It is possible that differences in the flow character of the in vivo model as well as host conditioning factors may have contributed to these differences in the rate of biofilm maturation. In addition, the high rate of development may be a function of the infecting inoculum used in these studies. A limitation of the present study is the absence of earlier time points to capture the initial periods of biofilm development. Future studies should include several earlier observations in the time course of in vivo development.

A unique feature of the present in vivo model is the ability to examine the impact of infection route in biofilm development. Several clinical investigators suggest that management of an intravascular catheter is of minimal consequence when the gastrointestinal tract is the source of candidemia, such as in patients with leukemia (40). However, the biofilm infection produced by a distant hematogenous infection route resulted in a biofilm structure indistinguishable from that resulting from direct catheter infection. Another result pointing to the importance of a catheter biofilm infection was the demonstration of metastatic infection of the renal parenchyma in animals with direct catheter infection. During catheter infection, care was taken to slowly instill the inoculum and to inject only the catheter volume. While it is possible or even likely that the *Candida* cells instilled in the catheter were released into the systemic circulation, cultures of peripheral blood within 10 to 20 min of direct infection did not grow on culture plates (data not shown). However, the relatively small volume (100  $\mu\text{l}$ ) cultured may not be sensitive enough to determine lower-level systemic candidemia.

Similar to results from a variety of assays used in in vitro models, these in vivo biofilms were resistant to the triazole antifungal fluconazole (3, 4, 8, 25, 34, 45, 47). Investigators have suggested that the lack of correlation between traditional

(planktonic) susceptibility testing results determined by NCCLS methods and clinical outcomes in patients with deep-seated *Candida* infections may be explained by the increased resistance of biofilms to antifungal drug therapy (46). The present in vivo study was limited to study of the impact of a single drug class on a preformed biofilm. Future studies should include study of addition drug classes as well as the impact of catheter pretreatment on biofilm prevention. It is difficult to compare the degree of drug resistance observed in vivo with that observed in vitro. Resistance to fluconazole has been reported to increase up to 4,000 times in in vitro-grown biofilm compared to planktonic cells (47). However, one could argue that it is similarly difficult to compare resistance among the in vitro studies, given the variability in assay methods. It is possible that the host immune system may act to reduce the impact of drug resistance. However, given the demonstration of the recalcitrance of these infections to antifungal therapy in patients, it is likely that drug resistance remains important in vivo. Given the suggestion of a larger biofilm matrix in this in vivo model discussed above, it is even possible that the in vivo biofilm is more drug resistant than biofilm in in vitro systems. However, one of the present in vitro assays measuring the MIC for dislodged biofilm-grown cells demonstrates a persistent resistance phenotype in the absence of matrix. The demonstration of persistent drug resistance in cells dislodged from the biofilm matrix has been previously shown with in vitro studies (3, 45). Possible additional resistance mechanisms have been identified in studies examining gene expression from in vitro biofilms. Recent studies have demonstrated that genes for both types of efflux pump (CDR and MDR) are upregulated during biofilm formation and development (34, 45). However, strains carrying single or double mutations of these genes retain a resistant phenotype during biofilm growth, demonstrating that additional, yet-unidentified resistance mechanisms are in play (45). In this study, we also investigated the mechanisms of *C. albicans* biofilm-associated fluconazole resistance at the genetic level. We observed increased expression of both the *CDR1* and *CDR2* genes in the in vivo biofilm cells compared to planktonically grown cells. However, we did not find an increase in the level of expression of the *MDR1* efflux pump, which was shown to be transiently upregulated prior to biofilm maturation (24 h) in vitro. A weakness of the present study was the limitation of these determinations to a single point in time (24 h), which in this model was associated with an architecturally mature biofilm. Similar to results from in vitro studies, we did not observe an increase in the abundance of mRNA from the fluconazole drug target, *ERG11*. Future study should include measurement of the entire transcriptome. In addition, this model would be useful for phenotypic study of mutations that have been examined and shown to be important with in vitro study, such as those genes associated with adherence and filamentation (8, 48, 56). We agree with the supposition that drug resistance in *C. albicans* biofilms, like that in bacterial biofilms, is complex and will not be explained by a single molecular mechanism (31). It will be similarly important to identify the genes associated with biofilm protection of cells from the host immune system, such as the monocyte/macrophage system.

There are numerous examples of differential gene expression in in vivo compared to in vitro test systems (16, 29, 54, 55, 60). A variety of in vivo bacterial infection models have been

used to investigate in vivo host-associated genotypic events. Recently, Lorenz and Fink have demonstrated the importance of similar observations in fungi by examining *C. albicans* gene expression associated with intracellular growth in macrophages (29). These investigations point to the relevance of genes associated with carbohydrate metabolism and suggest a number of potential future antifungal drug targets.

There have also been important examples of infection site-specific expression of specific genes *C. albicans* (35). Several investigators have demonstrated the expression and relevance of tissue-specific expression of members of the secreted aspartyl proteinase (SAP) family (35). Thus, examination of biofilm formation in a variety of infection sites, such as the urinary tract and joint space, should be explored.

In sum, factors that predispose organisms to adhere to device surfaces and contribute to the propagation of biofilms in vitro may not be the same factors that mediate this process in vivo at different sites of infection. To better understand and control biofilm infections, research must progress in a number of key areas. Among these is the development of models to more closely mimic host factors.

The present model provides a realistic model of the central venous catheter infection site, catheter-vascular flow, host conditioning protein and platelet conditioning, and the host immunity-biofilm interaction. We hope that more effective biofilm control strategies will result from research using in vivo models.

#### ACKNOWLEDGMENT

D. Andes is supported by NIH grant K08 AI 001767-04.

#### REFERENCES

- Anaissie, E. J., J. H. Rex, O. Uzun, and S. Vartivarian. 1998. Predictors of adverse outcome in cancer patients with candidemia. *Am. J. Med.* **104**:238–245.
- Bachmann, S. P., K. Vande Walle, G. Ramage, T. F. Patterson, B. L. Wickes, J. R. Graybill, and J. L. Lopez-Ribot. 2002. In vitro activity of caspofungin against *Candida albicans* biofilms. *Antimicrob. Agents Chemother.* **46**:3591–3596.
- Baillie, G. S., and L. J. Douglas. 1998. Effect of growth rate on resistance of *Candida albicans* biofilms to antifungal agents. *Antimicrob. Agents Chemother.* **42**:1900–1905.
- Baillie, G. S., and L. J. Douglas. 2000. Matrix polymers of *Candida* biofilms and their possible role in biofilm resistance to antifungal drugs. *J. Antimicrob. Chemother.* **46**:397–403.
- Baillie, G. S., and L. J. Douglas. 1999. Role of dimorphism in the development of *Candida albicans* biofilms. *J. Med. Microbiol.* **48**:671–679.
- Beck-Sague, C., and W. R. Jarvis. 1993. Secular trends in the epidemiology of nosocomial fungal infections in the United States, 1980–1990. *J. Infect. Dis.* **167**:1247–1251.
- Bustin, S. A. 2000. Absolute quantification of mRNA using real-time reverse transcription polymerase chain reaction assays. *J. Mol. Endocrinol.* **25**:169–193.
- Chandra, J., D. M. Kuhn, P. K. Mukherjee, L. L. Hoyer, T. McCormick, and M. A. Ghannoum. 2001. Biofilm formation by the fungal pathogen *Candida albicans*: development, architecture, and drug resistance. *J. Bacteriol.* **183**:5385–5394.
- Costerton, J. W., P. S. Stewart, and E. P. Greenberg. 1999. Bacterial biofilms: a common cause of persistent infections. *Science* **284**:1318–1322.
- Crnich, C. J., and D. G. Maki. 2002. The promise of novel technology for the prevention of intravascular device-related bloodstream infection. I. Pathogenesis and short term devices. *Clin. Infect. Dis.* **34**:1232–1242.
- Crump, J. A., and P. J. Collignon. 2000. Intravascular catheter-associated infections. *Eur. J. Clin. Microbiol. Infect. Dis.* **19**:1–8.
- Dato, V. M., and A. S. Dajani. 1990. Candidemia in children with central venous catheters: role of catheter removal and amphotericin B. *Pediatr. Infect. Dis. J.* **9**:309–314.
- Davey, M. E., and G. A. O'Toole. 2000. Microbial biofilms: from ecology to molecular genetics. *Microbiol. Mol. Biol. Rev.* **64**:847–867.
- Donlan, R. M., and J. W. Costerton. 2002. Biofilms: survival mechanisms of clinically relevant microorganisms. *Clin. Microbiol. Rev.* **15**:167–193.
- Donlan, R. M. 2001. Biofilm formation: a clinically relevant microbiological process. *Clin. Infect. Dis.* **33**:1387–1392.
- Dozois, C. M., F. Daigle, and R. Curtiss III. 2003. Identification of pathogen-specific and conserved genes expressed in vivo by an avian pathogenic *Escherichia coli* strain. *Proc. Natl. Acad. Sci. USA* **100**:247–252.
- Eppes, S. C., J. L. Troutman, and L. T. Gutman. 1989. Outcome of treatment of candidemia in children whose central catheters were removed or retained. *Pediatr. Infect. Dis. J.* **8**:99–104.
- Francois, P., P. H. Tu Quoc, C. Bisognano, W. L. Kelley, D. P. Le, J. Schrenzel, S. E. Cramton, F. Gotx, and P. Vaudaux. 2003. Lack of biofilm contribution to bacterial colonization in an experimental model of foreign body infection by *Staphylococcus aureus* and *Staphylococcus epidermidis*. *FEMS Immunol. Med. Microbiol.* **35**:135–140.
- Giacometti, A., O. Cironi, R. Ghiselli, L. Goffi, F. Mocchegiani, A. Riva, G. Scalise, and V. Saba. 2000. Efficacy of polycationic peptides in preventing vascular graft infection due to *Staphylococcus epidermidis*. *J. Antimicrob. Chemother.* **46**:751–756.
- Haugland, R. P. 1999. Handbook of fluorescent probes and research chemicals. Molecular Probes, Inc., Eugene, Oreg.
- Hawser, S. P., and L. J. Douglas. 1994. Biofilm formation by *Candida* species on the surface of catheter materials in vitro. *Infect. Immun.* **62**:915–921.
- Komshian, S. V., A. K. Uwayday, J. D. Sobel, and L. R. Crane. 1989. Fungemia caused by *Candida* species and *Torulopsis glabrata* in the hospitalized patient: frequency, characteristics, and evaluation of factors influencing outcome. *Rev. Infect. Dis.* **11**:379–390.
- Kuhn, D. M., J. Chandra, P. K. Mukherjee, and M. A. Ghannoum. 2002. Comparison of biofilms formed by *Candida albicans* and *Candida parapsilosis* on bioprosthetic surfaces. *Infect. Immun.* **70**:878–888.
- Leccione, J. A., J. W. Lee, E. E. Navarro, F. G. Witebsky, D. Marshall, S. M. Steinberg, P. A. Pizzo, and T. J. Walsh. 1992. Vascular catheter-associated fungemia in patients with cancer: analysis of 155 episodes. *Clin. Infect. Dis.* **14**:875–883.
- Lewis, R. E., D. P. Kontoyiannis, R. O. Darouiche, I. I. Raad, and R. A. Prince. 2002. Antifungal activity of amphotericin B, fluconazole, and voriconazole in an in vitro model of *Candida* catheter-related bloodstream infection. *Antimicrob. Agents Chemother.* **46**:3499–3505.
- Licking, E. 1999. Getting a grip on bacterial slime. *Business Week*, 13 September 1999, p. 98–100.
- Livak, K. J., and T. D. Schmittgen. 2001. Analysis of relative gene expression data using real-time quantitative PCR and the  $2^{-\Delta\Delta Ct}$  method. *Methods* **25**:402–408.
- Livak, K. J., S. J. Flood, J. Marmaro, W. Giusti, and K. Deetz. 1995. Oligonucleotides with fluorescent dyes at opposite ends provide a quenched probe system useful for detecting PCR product and nucleic acid hybridization. *PCR Methods Appl.* **4**:357–362.
- Lorenz, M. C., and G. R. Fink. 2001. The glyoxylate cycle is required for fungal virulence. *Nature* **412**:83–86.
- Luzzati, R., G. Amalfitano, L. Lazzarini, F. Soldani, S. Bellino, M. Solbiati, M. C. Danzi, S. Vento, G. Todeschini, C. Vivenza, and E. Concia. 2000. Nosocomial candidemia in non-neutropenic patients at an Italian tertiary care hospital. *Eur. J. Clin. Microbiol. Infect. Dis.* **19**:602–607.
- Mah, T. F., and G. A. O'Toole. 2001. Mechanisms of biofilm resistance to antimicrobial agents. *Trends Microbiol.* **9**:34–38.
- Maki, D. G., and P. A. Tambyah. 2001. Engineering out the risk of infection with urinary catheters. *Emerg. Infect. Dis.* **7**:1–6.
- Millard, P. J., B. L. Roth, H. P. Thi, S. T. Yue, and R. P. Haugland. 1997. Development of the FUN-1 family of fluorescent probes for vacuole labeling and viability testing of yeasts. *Appl. Environ. Microbiol.* **63**:2897–2905.
- Mukherjee, P. K., J. Chandra, D. M. Kuhn, and M. A. Ghannoum. 2003. Mechanism of fluconazole resistance in *Candida albicans* biofilms: phase-specific role of efflux pumps and membrane sterols. *Infect. Immun.* **71**:4333–4340.
- Naglik, J. R., G. Newport, T. C. White, L. L. Fernandes-Naglik, J. S. Greenspan, D. Greenspan, S. P. Sweet, S. J. Challacombe, and N. Agabian. 1999. In vivo analysis of secreted aspartyl proteinase expression in human oral candidiasis. *Infect. Immun.* **67**:2482–2490.
- National Committee for Clinical Laboratory Standards. 1997. Reference method for broth dilution antifungal susceptibility testing of yeasts. M-27A. National Committee for Clinical Laboratory Standards, Villanova, Pa.
- National Research Council Committee on the Care and Use of Laboratory Animals. 1996. Guide for the care and use of laboratory animals. National Academy Press, Washington, D.C.
- Nguyen, M. H., J. E. Peacock, D. C. Tanner, A. J. Morris, M. L. Nguyen, D. R. Snyderman, M. M. Wagener, and V. L. Yu. 1995. Therapeutic approaches in patients with candidemia. Evaluation in a multicenter, prospective, observational study. *Arch. Intern. Med.* **155**:2429–2435.
- Nucci, M., A. L. Colombo, F. Silveira, R. Richtmann, R. Salomao, M. L. Branchini, and N. Spector. 1998. Risk factors for death in patients with candidemia. *Infect. Control Hosp. Epidemiol.* **19**:846–850.
- Nucci, M., and E. Anaissie. 2002. Should vascular catheters be removed from all patients with candidemia? An evidence based review. *Clin. Infect. Dis.* **34**:591–599.

41. Pappas, P. G., J. H. Rex, J. D. Sobel, S. G. Filler, W. E. Dismukes, T. J. Walsh, and J. E. Edwards. 2003. Guidelines for treatment of candidiasis. *Clin. Infect. Dis.* **38**:161–189.
42. Potera, C. 1999. Forging a link between biofilms and disease. *Science* **283**:1837–1838.
43. Raad, I., M. F. Sabbagh, K. H. Rand, and R. J. Sherertz. 1992. Quantitative tip culture methods and the diagnosis of central venous catheter-related infections. *Diagn. Microbiol. Infect. Dis.* **15**:13–20.
44. Raad, I., W. Costerton, U. Sabharwal, W. Anaissie, and G. P. Bodey. 1993. Ultrastructural analysis of indwelling vascular catheters: a quantitative relationship between luminal colonization and duration of placement. *J. Infect. Dis.* **168**:400–407.
45. Ramage, G., S. Bachmann, T. F. Patterson, B. L. Wickes, and J. L. Lopez-Ribot. 2002. Investigation of multidrug efflux pumps in relation to fluconazole resistance in *Candida albicans* biofilms. *J. Antimicrob. Chemother.* **49**:973–980.
46. Ramage, G., K. Vande Walle, S. P. Bachmann, B. L. Wickes, and J. L. Lopez-Ribot. 2002. In vitro pharmacodynamic properties of three antifungal agents against preformed *Candida albicans* biofilms determined by time-kill studies. *Antimicrob. Agents Chemother.* **46**:3634–3636.
47. Ramage, G., K. Vande Walle, B. L. Wickes, and J. L. Lopez-Ribot. 2001. Standardized method for in vitro antifungal susceptibility testing of *Candida albicans* biofilms. *Antimicrob. Agents Chemother.* **45**:2475–2479.
48. Ramage, G., K. Vande Walle, J. L. Lopez-Ribot, and B. L. Wickes. 2002. The filamentation pathway controlled by the Efg1p regulator protein is required for normal biofilm formation and development in *Candida albicans*. *FEMS Microbiol.* **31**:95–100.
49. Ramage, G., K. Vande Walle, B. L. Wickes, and J. L. Lopez-Ribot. 2001. Characteristics of biofilm formation by *Candida albicans*. *Rev. Iberoam. Micol.* **18**:163–170.
50. Rex, J. H., J. E. Bennett, A. M. Sugar, P. G. Pappas, C. M. van der Horst, J. E. Edwards, R. G. Washburn, W. M. Scheld, W. A. Karchmer, A. P. Dine, et al. 1994. A randomized trial comparing fluconazole with amphotericin B for the treatment of candidemia in patients without neutropenia. *N. Engl. J. Med.* **17**:1325–1330.
51. Rex, J. H., J. E. Bennett, A. M. Sugar, P. G. Pappas, J. Serody, J. E. Edwards, and R. G. Washburn. 1995. Intravascular catheter exchange and duration of candidemia. *Clin. Infect. Dis.* **21**:994–996.
52. Rotrosen, D., T. R. Gibson, and J. E. Edwards, Jr. 1983. Adherence of *Candida* species to intravenous catheters. *J. Infect. Dis.* **147**:594.
53. Schmitt, M. E., T. A. Brown, and B. L. Trumppower. 1990. A rapid and simple method for preparation of RNA from *Saccharomyces cerevisiae*. *Nucleic Acids Res.* **18**:3091–3092.
54. Staib, P., M. Kretschmar, T. Michterlein, G. Kohler, S. Michel, H. Hof, J. Hacker, and J. Morschhauser. 1999. Host-induced, stage-specific virulence gene activation in *Candida albicans* during infection. *Mol. Microbiol.* **32**:533–546.
55. Staib, P., M. Kretschmar, T. Michterlein, H. Hof, and J. Morschhauser. 2002. Host versus *in vitro* signals and intrastrain allelic differences in the expression of a *Candida albicans* virulence gene. *Mol. Microbiol.* **70**:2758–2762.
56. Sundstrom, P. 2002. Adhesion in *Candida* spp. *Cell. Microbiol.* **4**:461–469.
57. Telenti, A., J. M. Steckelberg, L. Stockman, R. S. Edson, and G. D. Roberts. 1991. Quantitative blood cultures in candidemia. *Mayo Clin. Proc.* **66**:1120–1123.
58. Wey, S. B., M. Mori, M. A. Pfaller, R. F. Woolson, and R. P. Wenzel. 1988. Hospital-acquired candidemia. The attributable mortality and excess length of stay. *Arch. Intern. Med.* **148**:2642–2645.
59. White, T. C., K. A. Marr, and R. A. Bowden. 1998. Clinical, cellular, and molecular factors that contribute to antifungal drug resistance. *Clin. Microbiol. Rev.* **11**:382–402.
60. Xu, Q., M. Dziejman, and J. J. Mekalanos. 2003. Determination of the transcriptome of *Vibrio cholerae* during intrainestinal growth and midexponential phase *in vitro*. *Proc. Natl. Acad. Sci. USA* **100**:1286–1291.
61. Zimmerli, W., F. A. Woldvogel, P. Vaudaux, and U. E. Nydegger. 1982. Pathogenesis of foreign body infection: description and characteristics of an animal model. *J. Infect. Dis.* **146**:487–497.

Editor: T. R. Kozel